COMMUNICATIONS IN SCIENCE AND TECHNOLOGY
Homepage: cst.kipmi.or.id

Microwave-assisted biosynthesis of flower-shaped ZnO for photocatalyst in 4-nitrophenol degradation

Ari Sulistyo Rini[a,*], Arie Purnomo Aji[a], Yolanda Rati[b]

[a]*Department of Physics, Faculty of Mathematics and Natural Sciences, University of Riau, Riau 28293, Indonesia*
[b]*Department of Physics, Faculty of Mathematics and Natural Sciences, Bandung Institute of Technology, Bandung 40132, Indonesia*

Article history:
Received: 23 August 2022 / Received in revised form: 23 November 2022 / Accepted: 24 November 2022

Abstract

In this paper, the flower-shaped ZnO particles have been prepared via microwave-assisted biosynthesis technique using an aqueous extract of *Sandoricum koetjape* peel at various irradiation powers, i.e. 180, 360, 540, and 720 Watt. The synthesized flower-shaped ZnO particles were characterized using UV-Vis spectroscopy, x-ray diffraction (XRD), and field emission scanning electron microscope (FESEM). The UV-vis spectra exhibited ZnO absorption peaks in the UV region with band gap energy in the range of 3.25 - 3.29 eV. XRD analysis confirmed the hexagonal wurtzite crystal with the high purity of ZnO particles. The flower-shaped morphology of ZnO was evident in FESEM images with the decrease of particle diameter as the radiation power increased from 257 to 447 nm. ZnO prepared at 720 Watt (Z-720) succeeded in degrading 4-nitrophenol with the highest efficiency of 84.8 % after 240 min. Consequently, biosynthesis ZnO will have a great opportunity to be applied in degrading wastewater pollutants.

Keywords: 4-nitrophenol; microwave-assisted biosynthesis; flower-shaped; zinc oxide

1. Introduction

Industrial activities like mining, medicine, agriculture, and plantations discharge hazardous chemicals such as dye, disinfectant, heavy-metal, and pesticides into the environment. The phenolic compound is used extensively in the manufacturing of a broad variety of products, including medicines, fungicides, insecticides, and pigments[1]. 4-NP is a phenolic molecule with two functional groups (NO_2 and OH) on the benzene ring, which may disrupt ecosystems and harm human health [2]. 4-NP is a dangerous bio-refractory contaminant and considered as a high-priority pollutant that must be treated seriously[3].

Several methods such as coagulation, evaporation, carbon adsorption, and membrane filtration are commonly used in wastewater treatment. However, those methods still have limitation; for instance, some organic dyes are difficult to degrade, while others are not easily adsorbed and missed in the treatment process [4]. The semiconductor-based photo-degradation technique is an effective approach in the pollutants' decomposition [5]. In a photo-degradation process, when a semiconductor material is exposed to light with energy equal to or greater than its band gap energy, electron-hole pairs will be generated. The electron-hole pairs will then transform complex organic molecules into simple ones, such as CO_2 and H_2O[6].

Semiconductor such as TiO_2, ZnO, CdS, ZnS, SnO_2, Fe_2O_3, and GaP have been used as photocatalysts in organic degradation process [7]. However, of those semiconductor materials, ZnO has considerable high photocatalytic efficiency in degrading the pollutants because photogeneration efficacy to afford electron-hole pairs occurs rapidly [8]. In the scientific community, ZnO nanoparticles - due to their unique features such as semi-conductivity, opticality, antibacterial, antifungal, and high catalytic and photochemical activity – have become a concern. In addition, their low toxicity, biocompatibility, and biodegradability have made ZnO nanoparticles to be a desirable component for biomedicine and water purification systems [9].

Nanoparticle production mostly uses the physical and chemical methods that involve high temperatures, costly equipment, and hazardous substances [10]–[12]. Currently, a safe, fast, cost-effective synthesis technique with low energy use is required. Plant extract-based biosynthesis is more efficient for producing nanoparticles in comparison to physical and chemical methods. The adverse impacts of the resultant materials and their byproducts could be reduced by synthesizing nano-materials with biocompatible and eco-friendly chemicals.

Plants extracts such as Sea Buckthorn Fruit ZnO[13], Terminalia chebula fruits[14] and neem leaf extract[15] have been used to mediate the synthesis of ZnO nanoparticles (ZnO-NPs). Various biomolecules such as flavonoids, tannins, alkaloids, terpenoids, and antioxidants in plant extracts contribute to the reduction and stabilization of nanoparticles [16]. ZnO-NPs synthesized via a green synthesis technique also led to better antibacterial and photocatalytic activity [14], [15].

Controlling nanostructure shape and assembling into ordered microstructures are other strategies to generate more efficient functional materials [16]. ZnO with various

* Corresponding author.
Email: ari.sulistyo@lecturer.unri.ac.id
https://doi.org/10.21924/cst.7.2.2022.937

© 2022 KIPMI

nanostructures such as nanoflower [13], nanorod [17], and nanoreactor [18] have been reported to have superior performance in dye or pollutant degradation. E. Rupa et al. reported the ability of biosynthesized nanoflower ZnO to degrade 99% of industrial dye under UV-light within 70 minutes of contact time [13]. ZnO nanorod grown on glass substrate might degrade methylene blue up to 83% within 45 min [17]. In the photo-degradation of MO, ZnO nanoreactors demonstrated excellent heterogeneous photocatalytic properties with 10^3 times better efficiency than bulk ZnO [18].

Biosynthesis based on microwave (MW) heating might create nanostructured material with low energy consumption. Compared to conventional heating techniques, the microwave-biosynthesis approach may produce different-sized and -shaped metal oxide nanoparticles [19] and create nanoparticles with superior reaction rate and selectivity in photocatalysis [18], [20]. The dye removal efficiency of ZnO nanoparticles prepared via microwave irradiation method using Indian bael (Aegle marmelos) juice was 96% after 35 min of UV ($\lambda = 617$ nm) irradiation [21].

In this study, flower-shaped ZnO particles were synthesized using an aqueous extract of *Sandoricum koetjape (S. koetjape)* peel at various MW irradiation powers. MW irradiation powers were varied to investigate their impacts on the nanoparticle formation. *S. koetjape* peel extract was selected due to its strong antioxidant content with flavonoid components containing approximately 851.49 mg per 100 mg and polyphenols containing approximately 241.01 mg per 100 mg [22]. The optical, structural, and morphological properties of ZnO synthesized under different irradiation powers were analyzed. The photocatalytic activity of ZnO was investigated in degrading 4-NP pollutant.

2. Materials and Methods

2.1. Biosynthesis of ZnO particles

The synthesis procedure of ZnO using *S. koetjape* peel extract has been described in the previous report [23]. Typically, 40 mL of *S. koetjape* peel aqueous extract is mixed with zinc nitrate hexahydrate solution (0.2 M). The synthesis solution is then homogenized using a magnetic stirrer-bar and irradiated at various power (180, 360, 540 and 720 Watt) in a microwave oven for 3 minutes. The mixture is then left for 24 hours until forming precipitates. Thus, the precipitate was centrifuged at 4000 rpm for 10 minutes, washed three cycles in distilled water, and dried at 110°C. Each sample was designated as Z-xxx, where xxx represents the microwave irradiation power

2.2. Characterization

The optical properties were characterized using a UV-Vis SHIMADSU spectrophotometer with a wavelength range of 300-700 nm. The structure of ZnO was characterized using an X'Pert PRO type diffractometer at $\lambda_{Cu k\alpha} = 1.542$ Å. The surface morphology was investigated using a field emission scanning electron microscope (FESEM) model Quanta FEG 650 instrument at a magnification of 20,000x.

2.3. Photocatalyst experiments

The biosynthesized ZnO was evaluated in the degradation of 4-NP solutions under UV irradiation. A 20 mg of ZnO catalyst was dispersed in 4-NP with concentration 5 mg/L and then the NaOH solution was dropped until pH 12. The obtained solution was slightly stirred in the dark for about 60 min. The objective was to achieve a balance between adsorption and desorption between the 4-NP solution and photocatalyst surface. The UV-C lamp (237.5 nm) was employed as the light source. Small volumes (aliquots) were sampled periodically to monitor the decrease in the intensity of the 4-NP band at 400 nm using UV–Vis spectroscopy.

3. Results and Discussion

3.1. UV-Vis spectroscopy analysis

UV-Vis spectroscopy confirmed the formation of ZnO nanoparticles, as shown in Figure 1. The strong absorption band of ZnO occurred at the UV region wavelength up to 350 nm, 349 nm, 354 nm and 358 nm for the samples of Z-180, Z-360, Z-540, and Z-720, respectively. This result was consistent with the properties of ZnO exhibiting the maximum absorption at the wavelength near 360 nm [23]. The strong absorption band at roughly 360 nm was induced by host lattice absorption, implying the ability of UV light to stimulate ZnO NPs. The ability of electrons to absorb light at a certain wavelength caused absorption peaks to appear [21].

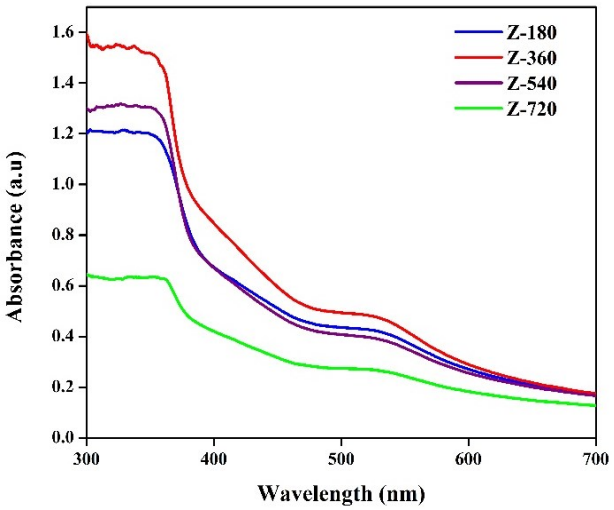

Fig. 1. UV-Vis Absorption spectrum of ZnO

The band gap energy of the ZnO was examined using the Tauc Plot method as shown in Fig 2. Band gap energy indicated the amount of photon energy absorbed by electrons (e^-) at the valence band excited to the conduction band and producing holes (h^+). Lower band gap energy facilitated the formation of e^- and h^+ pairs (exciton) that could reduce or oxidize toxic compound in photocatalysis reaction [24].

Samples Z-180, Z-360, Z-540, and Z-720 possessed the band gap energies of 3.29, 3.25, 3.26, and 3.28 eV, respectively. As the irradiation power increased, the band gap energy values decreased before increasing again. It was related to the size of the particles [20] where the small particles experienced quantum confinement, and nanocrystals contained distinct electronic stating that resemble molecules and display size-dependent characteristics [25]. As the crystal size decreased, the band gap tended to reduce (red-shift) to a

specific minimum value (critical size). When the size of the crystal was getting smaller compared to the minimum band gap size, and the trap moved to a higher energy level. This made the absorption spectrum blue-shifting (e.g., size quantization effect)[26].

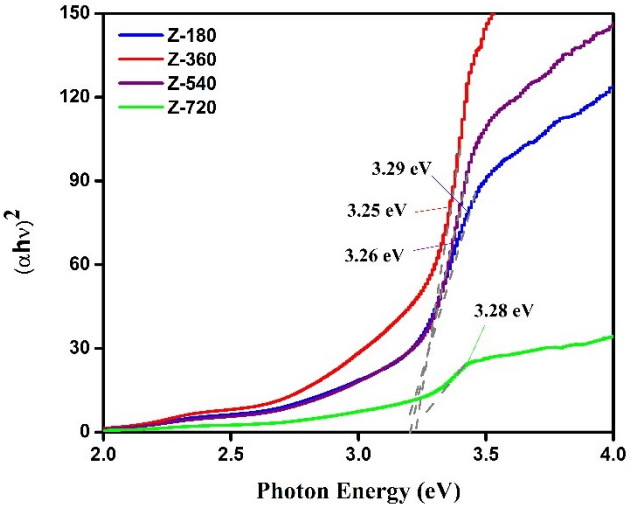

Fig. 2. The band gap energy of ZnO

3.2. XRD Analysis

The diffraction pattern of the ZnO samples is presented in Figure 3. The diffraction peaks of the ZnO at 2θ = 31°; 34°; 36°; 47°; 56°; 62°; 67° corresponded to (100), (002), (101), (012), (110), (013), (112) plane of hexagonal wurtzite crystal. The structure was analyzed using *Match3!* software database Crystallography Open Database no. 9008877. The sharp diffraction peaks indicated high crystallinity of biosynthesized ZnO without any impurity.

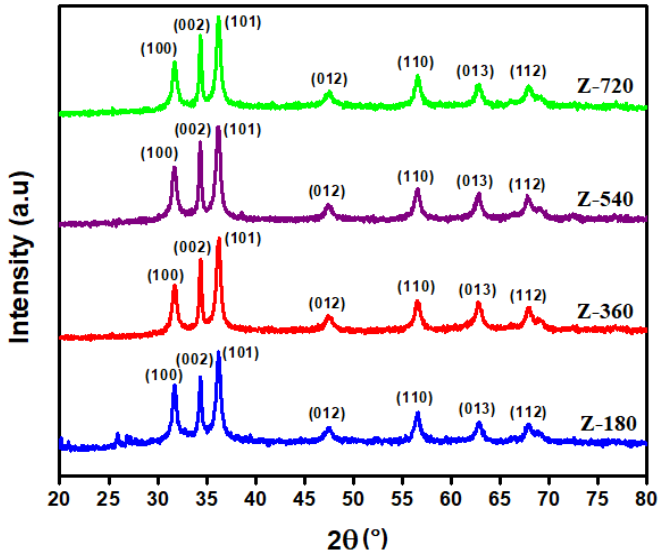

Fig. 3. Diffraction spectrum of biosynthesized ZnO at various irradiation power

Table 1 presents the lattice constant, crystallite size, and lattice strain of all samples. The average lattice parameters obtained were a = b = 3.25 Å and c = 5.22 Å. This value was found close to the previous report of biosynthesis ZnO using Moringa leaf extract, a = b = 3,21 Å and c = 5,26 Å [27].

Table 1. XRD parameter of ZnO samples

Samples	2θ (°)	Lattice constant		Crystallite	Lattice
		a (Å)	c (Å)	size (nm)	strain (Å)
Z-180	36.25	3.249	5.216	15.29	0.417
Z-360	36.22	3.246	5.238	15.71	0.406
Z-540	36.22	3.253	5.219	14.65	0.436
Z-720	36.24	3.250	5.215	15.55	0.411

Increasing the microwave power did not have such a large change in crystal size. The average crystal size of the ZnO was 15.3 nm with lattice strain of 0.417 Å.

3.3. Surface morphology

FESEM image was used to study the morphology of ZnO samples, as shown in Figure 4. The particles size was measured using imageJ and plotted in the histogram. In this case, the surface morphology of all samples tended to have uniform flower-shaped with different number of petals.

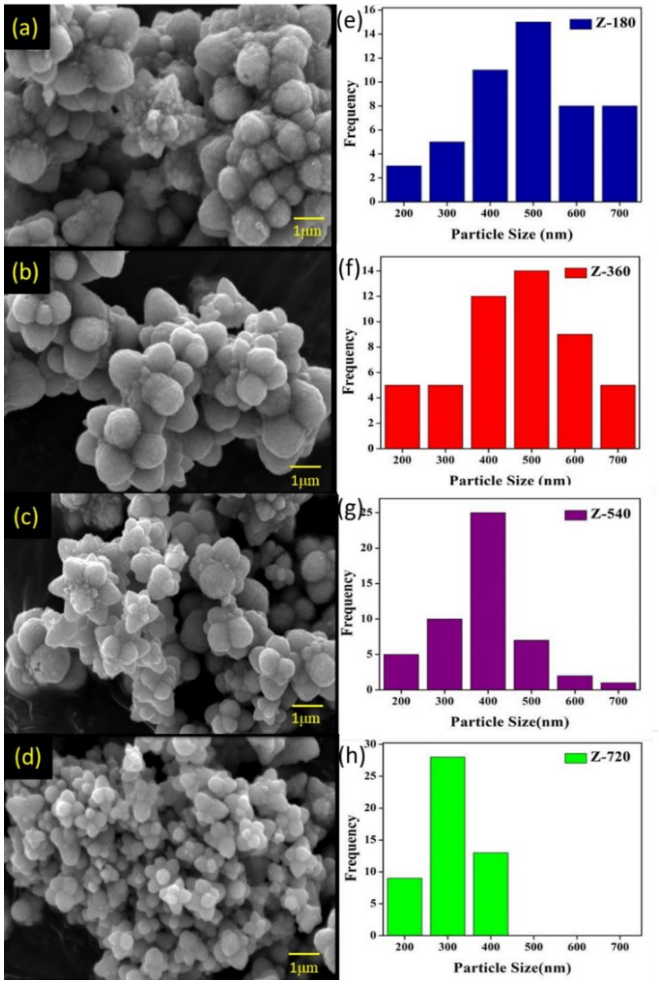

Fig. 4. Surface morphology and histogram of ZnO at various irradiation power (a) 180, (b) 360, (c) 540, and (d) 720 Watt

The Z-180 sample in Figure 4(a) showed particles in the shape of a flower with many petals. Sample Z-360 had fewer and bigger petals compared to sample Z-540. Nevertheless, sample Z-720, which was produced at a high irradiation power, had smaller, more uniform flower-like particles than other samples, as indicated by the histograms next to each sample. Greater microwave irradiation indicated that nanoparticle

production had become more homogeneous. In this study, the irradiation power also influenced the formation of nanoparticles [16].

The particle sizes were measured as the whole flower of ZnO particles. The average particle size of Z-180, Z-360, Z-540, and Z-720 were 447, 420, 338, and 257 nm, respectively. The ZnO particle size decreased as the irradiation power increases. Particle size also affected the ZnO's photocatalytic ability. The smaller the particle size, the larger the surface area obtained [28]. Surface area refers to an important factor for the degradation of organic pollutants as the number of active ions increases [29]. Because it has a homogeneous particle shape and size, Z-720, it is expected to have good photocatalytic ability.

3.4. Photocatalytic activity

Degradation of 4-nitrophenol (4-NP) was utilized as a model reaction to evaluate the ZnO photocatalytic activity. When the catalyst was introduced to the 4-NP solution, 4-nitrophenol was deprotonated to 4-aminophenolat (4-AP) [30]. The characteristic band of the phenolate group at 400 nm was recorded using UV-Vis. The degradation of contaminant was examined by using the highest absorbance of this band (A_0) as a reference and a way to monitor its drop as the reaction time elapsed, as shown in Figure 5. Table 2 presents the A/A_0 data at 30 min intervals and the reaction rate of each sample.

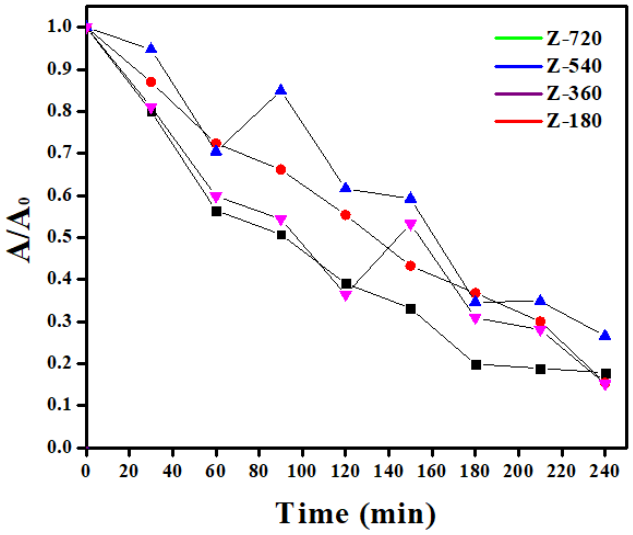

Fig. 5. 4-NP degradation using ZnO prepared at various irradiation power

Table 2. The A/A_0 data at 30 min intervals

Time (min)	Z-180	Z-360	Z-540	Z-720
0	1	1	1	1
30	0.8002	0.8699	0.9472	0.8105
60	0.5642	0.7238	0.7042	0.5981
90	0.5071	0.6614	0.8489	0.5439
120	0.3905	0.5537	0.6159	0.3641
150	0.3316	0.4323	0.5925	0.5324
180	0.1988	0.3679	0.3463	0.3089
210	0.1889	0.3002	0.3483	0.2807
240	0.1785	0.1545	0.2656	0.1520

After 240 minutes of reaction, the photodegradation efficiency of biosynthesized ZnO samples was estimated using the absorption peak reduction of 4-NP at 400 nm. The degradation efficiency of ZnO samples after 4 h from the highest and lowest, included Z-720, Z-180, Z-360 and Z540, respectively.

Table 3 presents the particle size, band gap energy, and photodegradation efficiency of ZnO samples. The 4-NP degradation efficiency for the Z-180 and Z-720 samples was 84.5% and 84.8%, respectively. Both samples had similar bandgap energy but are much different in particle size. Small particle will facilitate light absorption during the photocatalyst process and the large band gap energy value will avoid charge carrier recombination, which may reduce efficiency [34].

This present research has comparable results with previous research on 4-NP degradation using ZnO/GO doped zeolite nanocomposite material with a degradation efficiency of 82% [35].

Table 3. The particle size, band gap, photodegradation efficiency of ZnO at different power irradiation

Sample name	Particle size (nm)	Band gap (eV)	Photodegradation efficiency (%)
Z-180	447	3.29	84.5
Z-360	420	3.25	82.1
Z-540	338	3.26	73.2
Z-720	257	3.28	84.8

Previously, microwave-assisted biosynthesized ZnO had never been applied to degrade 4-NP. Therefore, ZnO prepared by this eco-friendly method can be developed in a wide range of pollutant degradation. Figure 6 depicts the photodegradation mechanism.

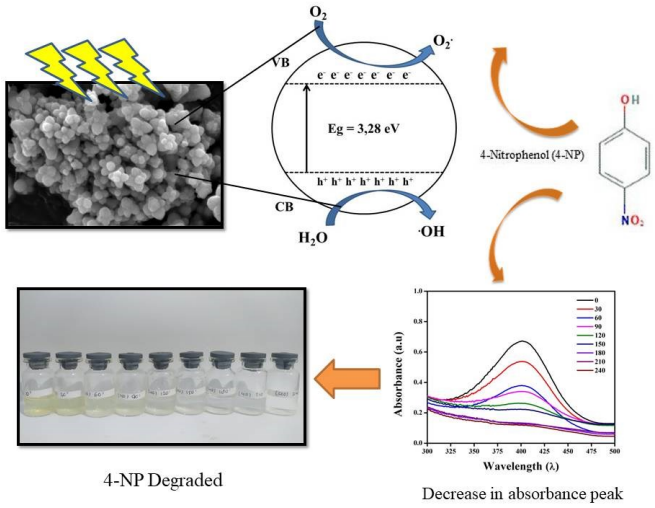

Fig 6. Photodegradation mechanism of biosynthesis ZnO

Photodegradation started when UV light hit ZnO with an energy greater than its band gap energy [31]. Electron-hole pair (exciton) would be created on the ZnO surfaces. Electron e^- and hole h^+ simultaneously reacted to O_2 and H_2O to create $^{\bullet}O_2$ and $OH^{\bullet}$ radicals, respectively. Both radicals were very reductive to change 4-NP molecules into colorless degraded molecules, H_2O dan CO_2. Therefore, as the photocatalytic reaction progresses, the yellow color of 4-NP degraded colorless[32].

4. Conclusion

In summary, flower-shaped ZnO particles were successfully conducted using a simple, effective, and eco-friendly biosynthesis approach. The effect of irradiation power has decreased the energy gap and enhanced the structural properties. As irradiation power increased, the size of ZnO

particles reduced and their distribution became more uniform. Therefore, these characteristics established the good properties of photodegradation of 4-NP pollutant.

Acknowledgements

The authors would like to thank the Directorate General of Research, Technology and Community Service, Ministry of Culture and Education, Republic of Indonesia and Institute for Research and Community Service, University of Riau that have financially supported and facilitated this research.

References

1. W. W. Anku, M. A. Mamo, and P. P. Govender, *Phenolic Compounds in Water: Sources, Reactivity, Toxicity and Treatment Methods*, Phenolic Compd. - Nat. Sources, Importance Appl. (2017) 419-443.
2. A. A. Yahya, K. T. Rashid, M. Y. Ghadhban, N. E. Mousa, H. S. Majdi, I. K. Salih, et al., *Removal of 4-nitrophenol from aqueous solution by using polyphenylsulfone-based blend membranes: Characterization and performance,* Membranes (Basel). 11 (2021) 1–20.
3. F. M. M. Tchieno and I. K. Tonle, *P-Nitrophenol determination and remediation: An overview*, Rev. Anal. Chem. 37 (2018) 1–26.
4. G. Crini and E. Lichtfouse, *Advantages and disadvantages of techniques used for wastewater treatment*, Environ. Chem. Lett. 17 (2019) 145–155.
5. F. Sadeghfar, Z. Zalipour, M. Taghizadeh, A. Taghizadeh, and M. Ghaedi, *Photodegradation processes*, Interface Science and Technology. 32 (2021) 55-124.
6. F. Opoku, K. K. Govender, C. G. C. E. van Sittert, and P. P. *Govender, Recent Progress in the Development of Semiconductor-Based Photocatalyst Materials for Applications in Photocatalytic Water Splitting and Degradation of Pollutants,* Adv. Sustain. Syst. 1 (2017) 1-24.
7. M. Yasmina, K. Mourad, S. H. Mohammed, and C. Khaoula, *Treatment heterogeneous photocatalysis; Factors influencing the photocatalytic degradation by TiO_2,* Energy Procedia. 50 (2014) 559–566.
8. A. A. McLain, *Photocatalytic Properties of Zinc Oxide and Graphene Nanocomposites*, Proc. Wisconsin Sp. Conf. 1 (2019) 1-5.
9. P. Rong, S. Ren, and Q. Yu, *Fabrications and Applications of ZnO Nanomaterials in Flexible Functional Devices-A Review*, Crit. Rev. Anal. Chem. 49 (2019) 336–349.
10. M. E. Fragalà, A. Di Mauro, D. A. Cristaldi, M. Cantarella, G. Impellizzeri, and V. Privitera, *ZnO nanorods grown on ultrathin ZnO seed layers: Application in water treatment*, J. Photochem. Photobiol. A Chem. 332 (2017).
11. A. K. Kapuscinska, M. Kwoka, M. A. Borysiewicz, M. Sgarzi, and G. Cuniberti, *ZnO Low-Dimensional Thin Films Used as a Potential Material for Water Treatment*, Eng. Proc. 6 (2021) 1-10.
12. T. A. Saleh, S. Majeed, A. Nayak, and B. Bhushan, *Principles and advantages of microwave- assisted methods for the synthesis of nanomaterials for water purification*, Adv. Nanomater. Water Eng. Treat. Hydraul. 16 (2017) 40–57.
13. E. J. Rupa, L. Kaliraj, S. Abid, D. C. Yang, and S. K. Jung, *Synthesis of a zinc oxide nanoflower photocatalyst from sea buckthorn fruit for degradation of industrial dyes in wastewater treatment,* Nanomaterials. 9 (2019) 1–18.
14. N. Rana, S. Chand, and A. K. Gathania, *Green synthesis of zinc oxide nano-sized spherical particles using Terminalia chebula fruits extract for their photocatalytic applications,* Int. Nano Lett. 6 (2016) 91–98.
15. M. J. Haque, M. M. Bellah, M. R. Hassan, and S. Rahman, *Synthesis of ZnO nanoparticles by two different methods & comparison of their structural, antibacterial, photocatalytic and optical properties*, Nano Express. 1 (2020) 1-14.
16. G. Manjari, S. Saran, S. Radhakrishanan, P. Rameshkumar, A. Pandikumar, and S. P. Devipriya, *Facile green synthesis of Ag–Cu decorated ZnO nanocomposite for effective removal of toxic organic compounds and an efficient detection of nitrite ions,* J. Environ. Manage. 262 (2020) 1-9.
17. L. Roza, V. Fauzia, and M. Y. Abd. Rahman, *Tailoring the active surface sites of ZnO nanorods on the glass substrate for photocatalytic activity enhancement Liszulfah*, Surfaces and Interfaces. 2019.
18. S. T. Tan, A. A. Umar, B. Aamna, N. Suratun, Y. Muhammad, C. Y. Chi, et al., *Ag − ZnO Nanoreactor Grown on FTO Substrate Exhibiting High Heterogeneous Photocatalytic Effi ciency*, ACS pubs. 16 (2014) 314–320.
19. J. Wojnarowicz, T. Chudoba, S. Gierlotka, and W. Lojkowski, *Effect of microwave radiation power on the size of aggregates of ZnO NPs prepared using microwave solvothermal synthesis,* Nanomaterials. 8 (2018).
20. A. Gupta, H. S. Bhatti, D. Kumar, N. K. Verma, and R. P. Tandon, *Nano and Bulk Crystal of ZnO: Synthesis and Characterization,* J. Nanomater. 1 (2006) 1–9.
21. C. Mallikarjunaswamy, V. Lakshmi Ranganatha, R. Ramu, Udayabhanu, and G. Nagaraju, *Facile microwave-assisted green synthesis of ZnO nanoparticles: application to photodegradation, antibacterial and antioxidant,* J. Mater. Sci. Mater. Electron. 31 (2020) 1004–1021.
22. N. Anantachoke, P. Lomarat, W. Praserttirachai, R. Khammanit, and S. Mangmool, *Thai fruits exhibit antioxidant activity and induction of antioxidant enzymes in HEK-293 cells,* Evidence-based Complement. Altern. Med. 2016 (2016) 1-14.
23. A. S. Rini, Y. Rati, and S. W. Maisita, *Synthesis of ZnO Nanoparticle using Sandoricum Koetjape Peel Extract as Bio-stabilizer under Microwave Irradiation,* J. Phys. Conf. Ser. 2049 (2021) 1-7.
24. D. A. Gopakumar, A. R. Pai, D. Pasquini, L. Shao-Yuan, H. P. S. Abdul Khalil, and S. Thomas, *Nanomaterials-State of Art, New Challenges, and Opportunities*. Elsevier Inc. 1 (2018) 1-24.
25. G. Ramalingam, *Quantum Confinement* (2020) 1–8.
26. L. E. Brus, *Electron-electron and electron-hole interactions in small semiconductor crystallites: The size dependence of the lowest excited electronic state,* J. Chem. Phys. 80 (1984) 4403–4409.
27. C. Sekhar, E. A. G. Rama, and K. Y. V Rami, *Green biosynthesis of ZnO nanomaterials and their anti - bacterial activity by using Moringa Oleifera root aqueous extract,* SN Appl. Sci. 2 (2020) 1–11.
28. A. Chafidz, A. R. Afandi, B. M. Rosa, J. Suhartono, P. Hidayat, and H. Junaedi, P*roduction of silver nanoparticles via green method using banana raja peel extract as a reducing agent,* Commun. Sci. Technol. 5 (2020) 112–118.
29. A. Kumar and G. Pandey, *A review on the factors affecting the photocatalytic degradation of hazardous materials*, Material Science & Engineering International Journal. 1 (2017) 106–114.
30. R. Trujillano, C. Najera, and V. Rives, *Activity in the Photodegradation of 4-Nitrophenol of a Zn,Al Hydrotalcite-Like Solid and the Derived Alumina-Supported ZnO,* Catal. MDPI. 10 (2020) 1–13.
31. A. S. Rini, A. Nabilla, and Y. Rati, *Microwave-assisted biosynthesis and characterization of ZnO film for photocatalytic application in methylene blue degradation,* Commun. Sci. Technol. 6 (2021) 69–73.
32. Sunaina, S. Devi, S. T. Nishanthi, S. K. Mehta, A. K. Ganguli, and M. Jha, *Surface photosensitization of ZnO by ZnS to enhance the photodegradation efficiency for organic pollutants*, SN Appl. Sci. 3 (2021).